Diabetologia (2002) 45:657–667
DOI 10.1007/s00125-002-0798-5

Diabetologia

An arginine to cysteine^{252} mutation in insulin receptors from a patient with severe insulin resistance inhibits receptor internalisation but preserves signalling events

I. Hamer[1], **M. Foti**[1], **R. Emkey**[3], **M. Cordier-Bussat**[4], **J. Philippe**[4], **P. De Meyts**[5], **C. Maeder**[1], **C. R. Kahn**[3], **J.-L. Carpentier**[1, 2]

[1] Department of Morphology, University of Geneva, Geneva, Switzerland
[2] Department of Morphology, CMU, Geneva, Switzerland
[3] Joslin Diabetes Research Center, Harvard Medical School, Boston, Massachusetts, USA
[4] Unit of Clinical Diabetology, University Cantonal Hospital, Geneva, Switzerland
[5] Hagedorn Research Institute, Gentofte, Denmark

Abstract

Aims/hypothesis. We examined the properties of a mutant insulin receptor (IR) with an Arg^{252} to Cys (IR^{R252C}) substitution in the α-subunit originally identified in a patient with extreme insulin resistance and *acanthosis nigricans*.
Methods. We studied IR cell biology and signalling pathways in Chinese Hamster Ovary cells overexpressing this IR^{R252C}.
Results. Our investigation showed an impairment in insulin binding to IR^{R252C} related mostly to a reduced affinity of the receptor for insulin and to a reduced rate of IR^{R252C} maturation; an inhibition of IR^{R252C}-mediated endocytosis resulting in a decreased insulin degradation and insulin-induced receptor down-regulation; a maintenance of IR^{R252C} on microvilli even in the presence of insulin; a similar autophosphorylation of mutant IR^{R252C} followed by IRS 1/IRS 2 phosphorylation, p85 association with IRS 1 and IRS 2 and Akt phosphorylation similar to those observed in cells expressing wild type IR (IRwt); and finally, a reduced insulin-induced Shc phosphorylation accompanied by decreased ERK1/2 phosphorylation and activity and of thymidine incorporation into DNA in cells expressing IR^{R252C} as compared to cells expressing IRwt.
Conclusion/interpretation. These observations suggest that: parameters other than tyrosine kinase activation participate in or control the first steps of IR internalisation or both; IR-mediated IRS 1/2 phosphorylation can be achieved from the cell surface and microvilli in particular; Shc phosphorylation and its subsequent signalling pathway might require IR internalisation; defective IR endocytosis correlates with an enhancement of some biological responses to insulin and attenuation of others. [Diabetologia (2002) 45:657–667]

Keywords Insulin receptor, endocytosis, insulin signalling.

Insulin receptor (IR) is a heterotetrameric glycoprotein composed of two extracellular α-subunits, containing the insulin binding sites, and two transmembrane β-subunits containing an intrinsic tyrosine kinase. Insulin binding to the α-subunit elicits a conformational change of the receptor resulting in activation of the β-subunit tyrosine kinase which, in turn, phosphorylates multiple endogenous proteins including the IR substrates (IRS 1 to 4), Shc and other cellular proteins [1, 2, 3, 4, 5, 6, 7, 8]. IRS and Shc serve as docking proteins for several specific signalling molecules [9].

Besides its role in signal transduction, insulin binding mediates a rapid internalisation of the newly formed ligand-receptor complexes by a redistribution of the IR from microvilli to the non-villous domains of the cell surface where they associate with the internalisation gates: the clathrin-coated pits [10]. This surface shift requires the activation of the tyrosine ki-

Received: 1 August 2001 / Revised: 21 December 2001
Published online: 5 April 2002

Corresponding author: J.-L. Carpentier, Department of Morphology, University of Geneva, Geneva, Switzerland, E-mail: Jean-Louis.Carpentier@medecine.unige.ch
Abbreviations: IR, Insulin receptor; IRwt, wild type insulin receptor; IR, ^{R252C} insulin receptor with an Arg 252 to Cys substitution; CHO, Chinese Hamster Ovary; EGF, epidermal growth factor; GST, glutathione S-transferase

nase as well as the phosphorylation of three specific tyrosines in the cytoplasmic domain whereas the association with clathrin-coated pits depends on several determinants in the β-subunit [10, 11]. Insulin-mediated internalisation modulates the number of IR expressed at the plasma membrane and allows the intracellular degradation of the hormone. So far, the role of IR internalisation on insulin signal transduction has remained controversial. On the one hand, several mutant IR have been shown to keep some of their functional properties although they failed to undergo insulin-induced internalisation [12, 13, 14, 15]. Likewise, under conditions where IR internalisation is inhibited (incubation at 4°C or expression of a dominant negative mutant of dynamin), IRS 1 is still phosphorylated [15, 16, 17], suggesting that IR internalisation is not required for the transduction of its biological signal. On the other hand, subcellular fractionation experiments (on 3T3-L1 adipocytes and rat hepatocytes) have shown that the pool of IR present on internal membranes undergoes a higher autophosphorylation in response to insulin than the IR present at the cell surface [18, 19], and that IRS 1 is mainly distributed in intracellular compartments, probably endosomes, where it could be tyrosine phosphorylated in the presence of insulin [16, 18, 19, 20]. These studies suggest therefore that IR signalling cascade takes place, at least in part, on endosomes and thus may require IR internalisation.

For many years, naturally occurring IR mutations have provided considerable information on the mechanisms of insulin action. In this study, we took advantage of such naturally mutated IR expressed in an insulin-resistant patient homozygous for the substitution of Arg^{252} with Cys in the α-subunit. Expression of this IR^{R252C} in CHO cells gave insights into the role of IR internalisation in its signalling in response to insulin binding.

Subject and methods

Subject. The patient was a 33-year-old man born from consanguine parents who suffered from a severe Type A syndrome of insulin resistance accompanied by *acanthosis nigricans*, hypertension, nephrotic syndrome and acromegaloid extremities [21]. All 22 exons of the IR gene were amplified by polymerase chain reaction and sequenced as previously reported [22]. Sequencing of genomic DNA revealed that the patient was homozygous for a point mutation in exon 3 with a Cys substituted for Arg^{252}.

Construction of IR^{R252C} by mutagenesis. The cDNA fragment containing the $^{252}Arg \rightarrow Cys$ mutation was obtained by site-directed mutagenesis using polymerase chain reaction. The PCR product was digested with *Kpn*I and *Eco*RI to yield a 398 bp fragment and substituted for the *Kpn*I/*Eco*RI segment (613–1011) of the wild-type IR cDNA. This construction was verified by nucleotide sequencing on both strands and subcloned into an expression vector in which the IR cDNA expression was driven by the CMV/T7 promoter.

Expression of IR^{R252C} in CHO cells. CHO cells (~750,000 cells) grown in Petri dishes (10 mm diameter) were transfected by the calcium precipitation technique with 5 µg of the expression vector containing the IR^{R252C} cDNA and 1 µg of a vector containing the neomycin resistance gene (pRSV-Neo). After selection for resistance to the antibiotic G418 (800 µg/ml) (Life Technologies, Basel, Switzerland), stable transfectants expressing the IR^{R252C} were cloned by fluorescence-activated cell sorter (Becton Dickinson FACScan, Basel, Switzerland). Briefly, cells were first incubated with biotinylated anti-IR antibody (1:500 in PBS/1% BSA) at 4°C and then with streptavidin R-phycoerythrin conjugate (1:20) (Caltag Lab, San Francisco, Calif., USA).

Insulin binding assay. CHO cells in 24-well plates were washed twice with phosphate-buffered saline (PBS) and incubated for 5 h at 4°C in Ham's F12 medium (Life Technologies, Basel, Switzerland) supplemented with 20 mM HEPES pH 7.4, 0.1% BSA, 21 pM ^{125}I-insulin and various known concentrations of unlabelled insulin. Thereafter, cells were washed twice with ice-cold PBS to remove unbound insulin and solubilised in 500 µl 0.1% SDS for 1 h. Cell-associated radioactivity was quantified in a γ-counter. Specific binding was determined by subtracting the amount of ^{125}I-insulin bound in the presence of excess (10^{-6} mol/l) unlabelled insulin. Insulin binding parameters were calculated with the LIGAND program [23].

Biosynthetic labelling and immunoprecipitation. CHO cells grown in 60 mm petri dishes were incubated in a methionine-free Eagle medium (Life Technologies, Basel, Switzerland) for 1 h at 37°C, pulse-labelled for 2 h in 1.2 ml of the same medium supplemented with 70 µCi Tran ^{35}S-label™ (ICN, Costa Mesa, Calif., USA), washed three times with phosphate-buffered saline (PBS) and chased for 3 h in 1.2 ml of complete Dulbecco's modified Eagle medium supplemented with 10% fetal calf serum. After the chase period, monolayers were washed with PBS and lysed for 30 min at 4°C in 1.2 ml of 50 mmol/l HEPES pH 7.4, 1% Triton X-100, 0.1% SDS, 1% sodium deoxycholate, 0.02% sodium azide, 21 µmol/l leupeptine, 23 mU aprotinin, 1 mmol/l EDTA and 0.2 mmol/l sodium iodoacetate [25].

IR were immunoprecipitated with a monoclonal antibody raised against the α-subunits of the IR (clone 83–14 from Neo-Markers, Union City, Calif., USA). Immunoprecipitates were washed twice with solution A (50 mmol/l HEPES pH 7.4, 120 mmol/l NaCl, 1% Triton X-100, 0.1% SDS, 1% sodium deoxycholate), once with solution B (PBS pH 7.4, 0.5% BSA, 1% Triton X-100, 0.5% sodium deoxycholate, 2 mol/l KCl) and twice with solution A. Eventually, samples were dissolved in Laemmli buffer and analysed by SDS-PAGE (7.5%) under reducing conditions. Gels were subjected to autoradiography for 3 days. Autoradiographic films were analysed by densitometry (ImageQuant, Molecular Dynamics, Dübendorf, Switzerland).

Cell surface expression of biotinylated IR. Confluent monolayers of CHO cells were grown up in Petri dishes (10 mm diameter). Cell surface proteins were biotinylated as previously described [24]. Briefly, cells were incubated in dPBS (Life Technologies) containing 0.5 mg/ml N-hydroxysuccinimide long chain biotin (NHS-LC-biotin, Pierce, Rockford, Ill., USA) for 30 min at 4°C. Cells were then incubated in 5 ml of binding buffer in the absence or presence of 10^{-7} mol/l insulin for 1 min at 37°C. Cells were washed and solubilised in 800 µl lysis buffer containing protease inhibitors. IR were immunoprecipitated, separated by SDS-PAGE (6.5%) and blotted onto nitrocellulose sheets. Bands corresponding to cell surface IR

were detected with horseradish peroxidase-linked streptavidin (Amersham Biosciences, Dübendorf, Switzerland). After extensive washes, enhanced chemiluminescence (ECL kit, Amersham Biosciences) detection was performed according to the manufacturer's instructions (Amersham Biosciences).

Constitutive and insulin-induced internalisation of IR in CHO cells. Confluent monolayers of transfected CHO cells were first incubated for 2 h at 4°C in the presence of 5 pmol/l ^{125}I-mAb 83–14 (constitutive internalisation) or 50 pmol/l ^{125}I-insulin (insulin-induced internalisation) then transferred to 37°C for various periods of time. At each time point studied, the unbound ^{125}I-ligand was removed and cells were washed three times with ice-cold phosphate-buffered saline (PBS). Cells were then subjected to three 5-min washes with ice-cold PBS at pH 1.5 to release the ^{125}I-ligand bound at the cell surface. Finally, cells were lysed in 1 N NaOH and all samples (acid washes and lysates) were counted in a Beckman 5500 γ-counter to determine the internalised radioactivity *versus* total radioactivity.

Downregulation of IR. CHO cells were maintained overnight in a F12 medium containing 10^{-7} mol/l unlabelled insulin and then incubated for 2 h at 4°C in the presence of a tracer amount of ^{125}I-insulin. After three washes, the amount of ^{125}I-insulin bound to the cell surface was measured on cell lysates with a Beckman 5500 γ-counter.

Insulin degradation. CHO cells, grown in 35 mm-Petri dishes, were incubated for 2 h at 4°C in the presence of a tracer amount of ^{125}I-insulin and then transferred at 37°C. After various time periods, culture medium was collected, the insulin-bound to the plasma membrane was recovered by three acid washes and cells were lysed in 0.1% Triton X100, 3 mol/l acetic acid and 6 M urea. ^{125}I-insulin molecules were precipitated with 10% trichloroacetic acid and the radioactivity associated with the pellets were quantified with a Beckman 5500 γ-counter.

Autophosphorylation of IR and phosphorylation of pp185. Subconfluent CHO cells grown in 100 mm culture dishes were serum-starved for 16 h at 37°C in Ham's F12 medium containing 20 mmol/l HEPES pH 7.6. After biotinylation of cell surface proteins, cells were incubated for 1 min at 37°C in the same medium supplemented or not with various concentrations of insulin. After removal of the medium, cells were frozen in liquid nitrogen and lysed with 800 µl of lysis buffer (50 mmol/l HEPES pH 7.4, 150 mmol/l NaCl, 1% Triton X-100, 2 mmol/l ortho-vanadate, 4 mmol/l sodium pyrophosphate, 0.1 mol/l NaF) containing 10 µg/ml pepstatin, 1 mmol/l PMSF and 62.5 µg/ml aprotinin. Lysates were centrifuged at 1200 g for 30 min to discard cell debris. IR were immunoprecipitated as described above and isolated by SDS-PAGE. Phosphorylated IR were detected by immunoblotting using an anti-phosphotyrosine antibody (4G10 from Upstate Biotechnology, Lake Placid, N.Y., USA) and visualised by enhanced chemiluminescence (Amersham Biosciences). Thereafter, the nitrocellulose sheets were cleaned with 0.1 mol/l glycine pH 3/0.1 mol/l NaCl and probed with streptavidin-peroxidase to detect the cell surface IR.

The same procedure was followed to study the phosphorylation of pp185 (=IRS 1 and IRS 2), except that cells were incubated for 2 min at 37°C in the presence of insulin instead of 1 min. 25 µg of proteins were loaded onto a 10% SDS acrylamide gel and phosphorylated proteins were detected as described above.

Phosphorylation of insulin substrates. Serum-starved CHO cells were incubated for 3 min in the presence of 10^{-7} mol/l insulin and lysed as described above. IRS-1, IRS-2 and Shc were immunoprecipitated with the appropriate antibodies and phosphorylated proteins were detected with the antiphosphotyrosine antibody 4G10 (Upstate Biotechnology) after SDS-PAGE and electrophoretic transfer onto a nitrocellulose sheet.

Measurement of p85 binding to IRS1/2 by far-Western blotting. Cells, incubated or not with 10^{-7} mol/l insulin, were subjected to phosphotyrosine immunoprecipitation, separated on SDS-PAGE, transferred to nitrocellulose, blocked and incubated with either GST (glutathione S-transferase) or GST-nSH_2p85, a fusion protein made of GST and the amino terminal SH_2 domain of p85. The blots were then subjected to anti-GST immunoblot analysis.

Akt and ERK1/2 phosphorylation and activity. Serum-starved CHO cells were incubated for the indicated times with 10^{-7} mol/l insulin at 37°C, washed in cold PBS, and lysed in 50 mmol/l HEPES pH 7.8, 1% Triton X-100, 2.5 mmol/l EDTA, 10 mmol/l $Na_4P_2O_7$, 100 mmol/l NaF, 2 mmol/l ortho-vanadate and protease inhibitors. Lysates were centrifuged at low speed to discard cell debris and nucleus and equal amount of proteins were loaded on 10% SDS acrylamide gels. Phosphorylated Akt, total Akt, phosphorylated ERK1/2 and total ERK1/2 were detected by Western blot analysis using specific antibodies from Cell Signalling (Beverly, Mass., USA). ERK1/2 activity was determined using the p44/42 MAP Kinase Assay kit from Cell Signalling (Beverly) according to the manufacturers instructions.

[^{3}H] Thymidine incorporation into DNA. Near-confluent cells were grown in 24-well plates were serum-starved for 36 h at 37°C in Ham's F12 medium. Thereafter, the medium was removed and replaced with RPMI 1640 containing 20 mM HEPES, 0.1% BSA and supplemented with various known concentrations of insulin. After incubation for 15 h at 37°C, 0.5 µCi/well [methyl-^{3}H] thymidine (specific activity: 46 Ci/mmol, Amersham Biosciences) in Ham's F12 medium was added without washing and incubated for another 2 h at 37°C. Cells were washed three times with ice-cold PBS containing 1 mmol/l $CaCl_2$ and 1 mmol/l $MgCl_2$ and then lysed in 1 ml 0.1% SDS for 2 h at 4°C. After addition of 1 ml of 20% trichloroacetic acid, the lysates were centrifuged at 1800 g for 30 min. The pellets were dissolved in 0.3 ml 1 N NaOH and neutralised with 0.1 ml 3 N HCl. Radioactivity was quantified with a β counter on 100 µl samples in the presence of 3 ml of scintillation liquid (Beckman Instruments, Nyon, Switzerland).

Statistical analysis. Results are expressed as mean ± SEM. Comparisons were made by using the Student's *t* test. Differences were considered as significant at $p<0.05$ (*) or $p<0.01$ (**).

Results

Insulin binding to IR^{R252C}. A study carried out 18 years ago on erythrocytes isolated from a patient with a Type A syndrome of insulin resistance, revealed that these cells exhibited a 40% decrease in IR on the cell surface and a fivefold decrease in ^{125}I-insulin binding affinity when compared to cells from a healthy individual (unpublished observations). Scatchard analyses showed a dissociation constant (Kd) for insulin of

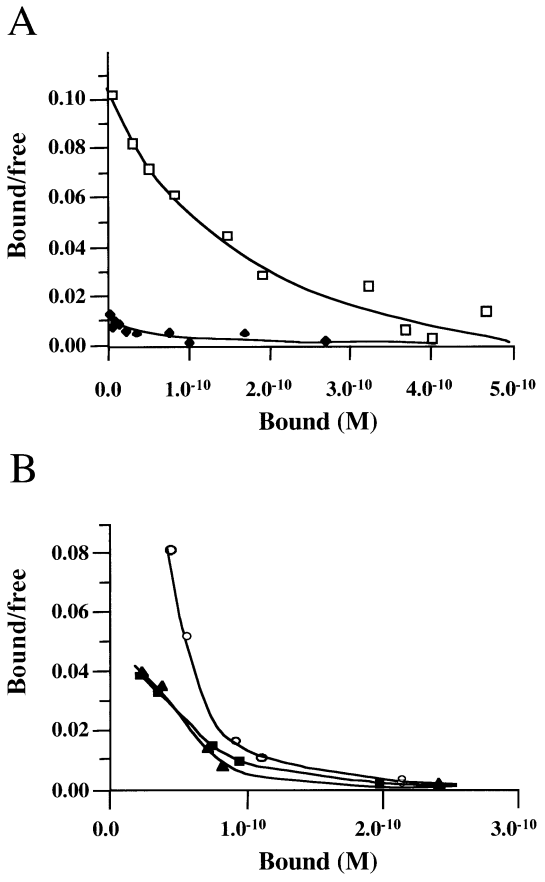

Fig. 1A, B. Scatchard plots of insulin binding. **A** Results obtained on erythrocytes from the patient (*diamonds*) and a healthy individual (*open squares*). **B** Results obtained on CHO cell lines expressing the IRwt (*open circles*) and the IR^{R252C} mutant receptor (clones C3, *solid squares* and E6, *solid triangles*). Cells were plated on 24-well plates and incubated for 5 h at 4°C in the presence of ^{125}I-insulin and the indicated concentrations of unlabelled insulin. Radioactivity bound to the cell surface was evaluated with a γ-counter after two washes with PBS/BSA

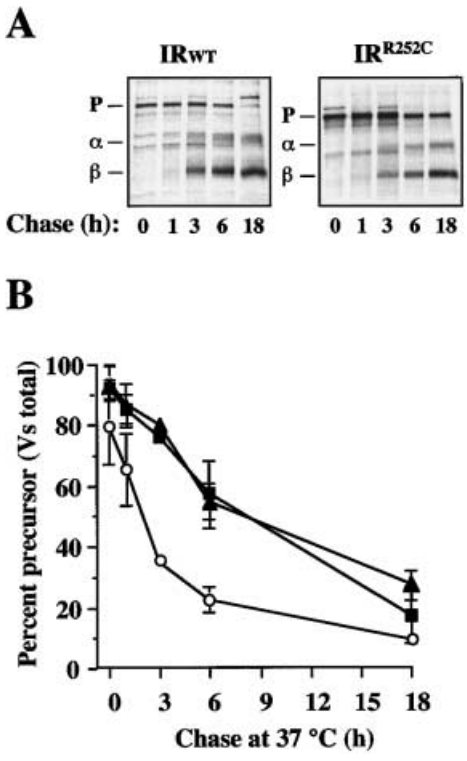

Fig. 2A, B. Biosynthetic labelling of IR in transfected CHO cells. **A** Cells expressing the wild-type IR (IRwt, *left panel*) or the IR^{R252C} mutant receptor (clone E6, *right panel*) were pulse-labelled for 2 h with Tran ^{35}S label and then chased for the indicated periods in a complete unlabelled culture medium. IR were immunoprecipitated and analysed by SDS-PAGE and subsequent autoradiography. *P*, precursor; α, α-subunit of IR; β, β-subunit of IR. **B** Densitometric analysis of three independent experiments; IRwt (*open circles*), IR^{R252C} clone E6 (*solid triangles*), IR^{R252C} clone C3 (*solid squares*)

25 and 5 nmol/l in cells from the diabetic patient and healthy subject, respectively (Fig. 1A).

From the genomic DNA of the patient, we amplified all 22 exons of the IR gene by polymerase chain reaction and sequenced them. We identified a point mutation in codon 252 of exon 3 (C to T) resulting in the change of amino acid 252, from an arginine to a cysteine. In the absence of DNA from the proband's parents, genotypes were determined for seven polymorphic loci (all microsatellites) on chromosome 19; the finding of homozygosity for four polymorphic markers on chromosome 19p, including and distal to *IR* gene, supports homozygosity by inbreeding for the *IR* gene mutation.

To further characterise the consequence of this point mutation on the functioning of the receptor and on insulin action, both normal and mutant *IR* cDNA were transfected into CHO cells and stable clones selected. Two clones expressing IR^{R252C} (clones C3 and E6) and a clone expressing the wild type IR (IRwt) were used throughout this study.

As shown by Scatchard plot analysis, the ^{252}Arg→Cys mutation is accompanied by a reduction in the affinity of the IR for insulin. The Kd values were 6.9 and 5.0 nmol/l respectively for the clones C3 and E6 as compared to 1.8 nmol/l for IRwt. These observations are in agreement with the experiment carried out on freshly isolated erythrocytes from the patient (see above).

Biosynthetic labelling and cell surface expression of IR^{R252C} in CHO cells. To investigate whether the reduced affinity of IR^{R252C} for insulin resulted from a misprocessing of the receptor, cells were metabolically pulse-labelled for 2 h with Tran ^{35}S label and then chased for increasing periods of time. After the pulse period, the major band that appeared corresponds to the precursor (190 kDa) (Fig. 2A). Then, two other bands, corresponding to the immature α (120 kDa) and β (85 kDa), appeared after 3 h of chase, indicating that the precursor is properly cleaved into the α- and β-subunits. However, a densitometric analysis indicat-

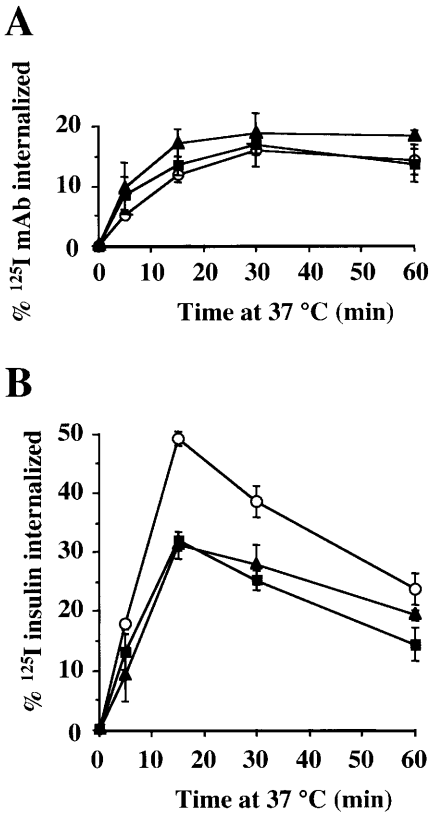

Fig. 3A, B. Constitutive and insulin-induced internalisation of IR in CHO cells. Subconfluent monolayers of CHO cells expressing the IRwt (*open circles*) or the IR^{R252C} mutant (clones C3, *solid squares* and E6, *solid triangles*) were incubated at 4°C for 2 h in the presence of a tracer amount of ^{125}I-mAb (**A**) or of ^{125}I-insulin (insulin-induced internalisation, (**B**) and then washed and warmed at 37°C. After the indicated periods of time, cells were washed with acid PBS to remove the unbound ligand and lysed to determine the amount of internalised IR. Results are expressed as means ± SE of three independent experiments

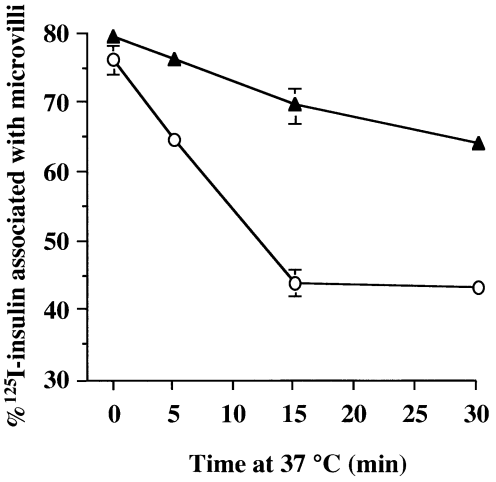

Fig. 4. Surface redistribution of IR in CHO cells. CHO cells expressing the IRwt (*open circles*) and the IR^{R252C} mutant (clone E6, *solid triangles*) cell lines were incubated at 37°C in the presence of ^{125}I-insulin for the indicated periods of time and further processed for EM autoradiography. Results represent the percentage of the total number of autoradiographic grains associated with the cell surface (±250 nm from the plasma membrane) whose centres were within a distance of 250 nm from microvilli (n=3)

ed that the disappearance of IR^{R252C} precursor and its maturation into α- and β-subunits were delayed as compared to IRwt (Fig. 2B).

To determine which form of IR^{R252C} was expressed at the plasma membrane, the cell surface proteins were labelled with NHS-LC-biotin, IR were immunoprecipitated and the IR present at the plasma membrane were detected with horseradish-linked streptavidin. Similarly to IRwt receptors, the IR^{R252C} appeared exclusively under the $\alpha_2\beta_2$ processed form (data not shown).

Internalisation of IR^{R252C} and its consequences on IR^{R252C} downregulation and insulin degradation. ^{252}Arg→Cys mutation did not affect the constitutive internalisation of the IR as measured using a ^{125}I-labelled monoclonal antibody to the receptor (Fig. 3A). By contrast, insulin-stimulated internalisation of the IR^{R252C} was reduced compared to that of IRwt (Fig. 3B). As determined by quantitative electron microscopic analysis of ^{125}I-insulin localisation on CHO cells expressing IR^{R252C}, this internalisation defect was related to a defective redistribution of the IR^{R252C} from microvilli to the non-villous regions of the cell surface where internalisation takes place (Fig. 4).

The reduced internalisation of the IR^{R252C} led to a marked reduction in the degradation of the internalised ^{125}I-insulin (Fig. 5A) and to an increase in the residual ^{125}I-insulin binding at the cell surface (Fig. 5B). These observations suggest that the ^{252}Arg→Cys mutation in the α-subunit of IR reduces the surface mobility of the receptor and subsequently leads to an impaired internalisation of ligand-receptor complexes and an inhibition of both IR^{R252C} down-regulation and insulin degradation.

Insulin-induced activation of IR and downstream pathways. In spite of a reduction in affinity of IR^{R252C} as compared to IRwt (see above), exposure of CHO cells bearing the IR^{R252C} mutant (clones C3 and E6) to 10^{-7} mol/l insulin for 1 min resulted in a marked tyrosine phosphorylation of IR^{R252C} β-subunit (Fig. 6A). When expressed as percent of maximal phosphorylation, the dose-response curves for receptor autophosphorylation of cells expressing IR^{R252C} and IRwt were similar (Fig. 6B). The evolution of receptor autophosphorylation as a function of the incubation time was also similar for the wild type IR and the IR^{R252C} mutant (Fig. 6C).

Likewise, Western blot analysis using an anti-tyrosine phosphoprotein antibody following stimulation by different concentrations of insulin revealed similar, or slightly higher, phosphorylation of the pp185 pro-

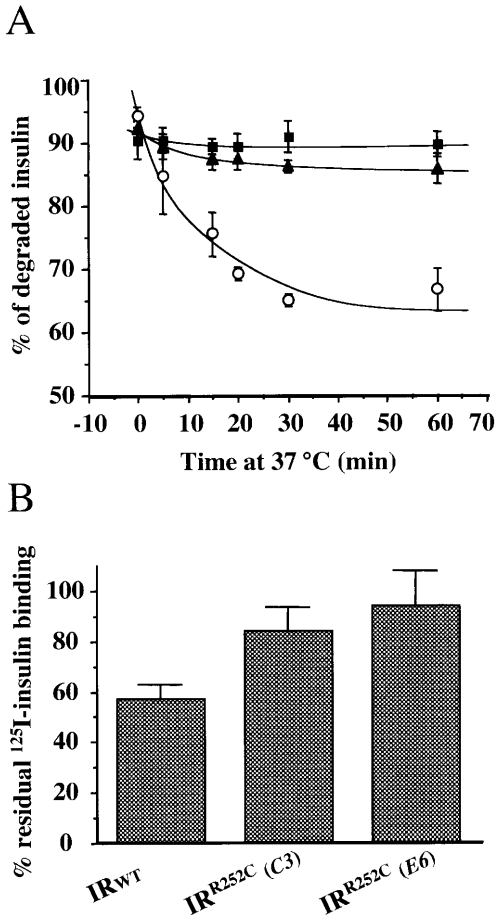

Fig. 5A, B. Insulin degradation and residual ^{125}I-insulin binding following down-regulation of IR in CHO cells. **A** Cells expressing the IRwt (*open circles*) and the IR^{R252C} mutant (clones C3, *solid squares* and E6, *solid triangles*) were incubated at 4°C for 2 h in the presence of a tracer amount of ^{125}I-insulin and then warmed at 37°C. After the indicated times, cell samples and culture media were subjected to TCA precipitation to estimate the amount of ^{125}I-insulin molecules remaining intact after the incubation at 37°C. Results represent the percent of degraded ^{125}I-insulin versus ^{125}I-insulin recovered inside the cells and in the culture medium (means ± SE, *n*=3). **B** Cells were incubated overnight in the absence (control) or in the presence of 10^{-7} mol/l insulin and then exposed to ^{125}I-insulin for 2 h at 4°C. Results are expressed in percent of residual binding at the end of the 2 h incubation at 4°C and represent the mean of three individual experiments (± SEM)

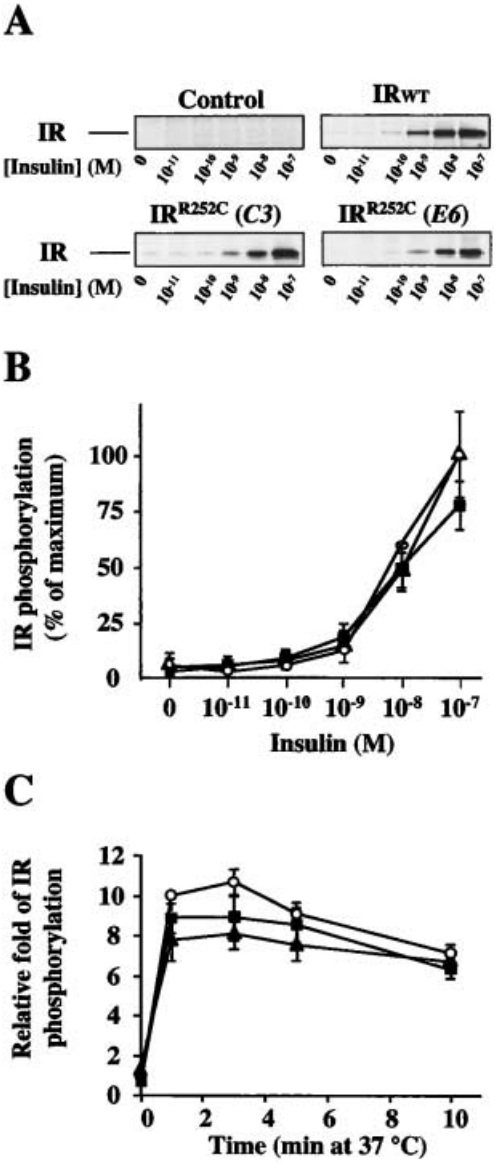

Fig. 6A–C. Autophosphorylation of IR. **A** Cells were serum-starved for 12 h and IRwt or IR^{R252C} mutant were immunoprecipitated by an antibody against the α-subunit, resolved by SDS-PAGE and further analysed by immunoblotting using an anti-phosphotyrosine antibody. CHO cells expressing endogenous levels of IR were used as a control. **B** Densitometric analysis of three independent experiments. **C** Kinetics of phosphorylation of IRwt and IR^{R252C} mutant in CHO cells. IRwt (*open circles*), IR^{R252C} clone E6 (*solid triangles*), IR^{R252C} clone C3 (*solid squares*)

teins (including IRS 1 and IRS 2) in cells expressing IR^{R252C} than in cells expressing IRwt (Fig. 7A). When the respective phosphorylation of IRS 1 and IRS 2 were separately analysed, no difference was noted between the ability of these two substrates to be phosphorylated in response to insulin in cells expressing the IRwt or the IR^{R252C} mutant (Fig. 7B). Then, we analysed two downstream effectors of IRS proteins in the metabolic pathways stimulated by insulin: PI3 kinase and Akt/PKB (a serine-threonine kinase whose activity depends upon PI3 kinase [26]). In cells expressing IR^{R252C}, insulin stimulated the association of the regulatory (p85) subunit of PI3 kinase with IRS1 and IRS2 (Fig. 7C) and the phosphorylation of Akt (Fig. 7D), similarly than in cells expressing IRwt. In contrast, the insulin-induced phosphorylation of the p52 Shc isoform, another major initial substrate of the IR in pathways directing the mitogenic effect of insulin, was reproducibly reduced (by 27 to 38 percent) in cell expressing the IR^{R252C} mutant as compared to cells expressing the wild type IR (Fig. 8A). These changes were not accompanied by any alteration in Shc isoform distribution and in Shc protein expression

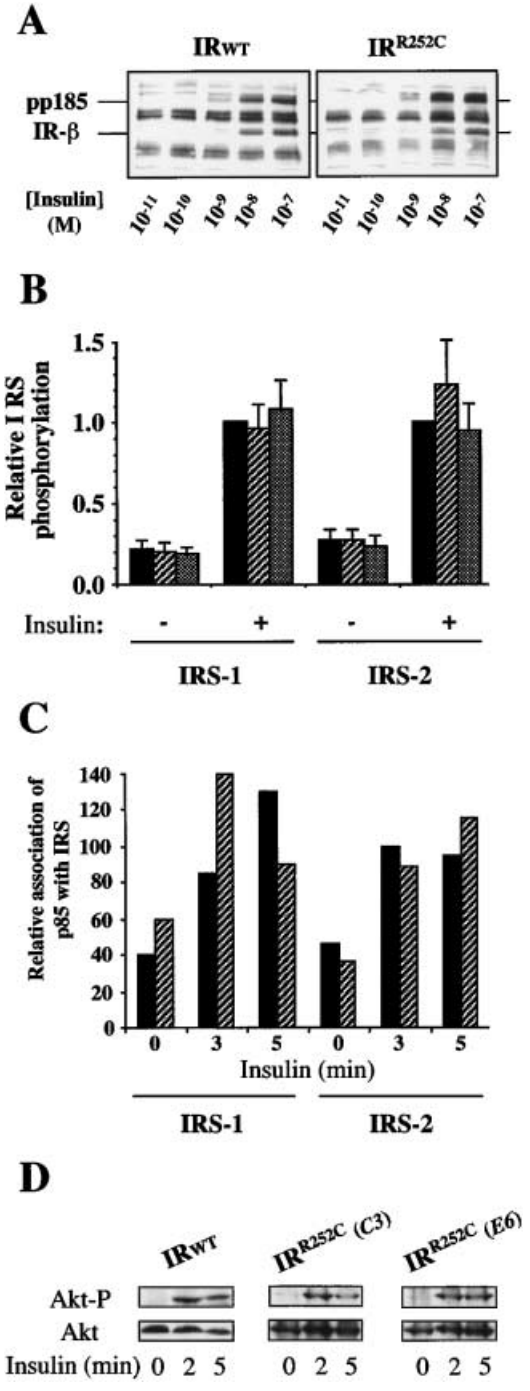

Fig. 7A–D. Insulin-induced phosphorylation of IRS 1, IRS2 and Akt/PKB. **A** Tyrosine-phosphorylation of pp185. Cells expressing the wild-type IR or the IR^{R252C} mutant (clone E6) were incubated with insulin, lysed and analysed by SDS-PAGE and Western blotting using an anti-phosphotyrosine antibody. **B** Phosphorylation on IRS-1 and IRS-2. Cells expressing the wild-type IR (*solid bars* IRwt) or the IR^{R252C} mutant (clones C3, *forward hatched bars* and E6, *grey bars*) were incubated with 10^{-7} mol/l insulin and tyrosine phosphorylation of IRS 1 or IRS 2 were quantified by densitometric analysis of Western blots. Results are expressed as mean ± SE of 6 independent experiments. **C** IRS1/2 association with PI 3-kinase. Association of IRS-1 and IRS-2 with the p85 subunit of the PI3-kinase was assessed in IRwt (*solid bars* IRwt) and IR^{R252C} mutant (clone C3, *forward hatched bars*) expressing cells using an overlay assay. **D** Akt phosphorylation. Cells expressing the IRwt or the IR^{R252C} mutant were treated with 10^{-7} mol/l insulin and Akt phosphorylation was analysed as described in the Methods section

in cells expressing the various forms of IR under study (data not shown). To further track the alterations which might concern the Shc signalling pathway, ERK1/2 phosphorylation and activation in response to insulin were analysed. The mutation R252C led to a marked reduction in the phosphorylation of ERK1/2 and of Elk-1 (a substrate of ERK1/2) (Fig. 8B and C). Eventually, we investigated the rate of DNA synthesis after a long exposure of CHO cells to various concentrations of insulin. In cells expressing the IR^{R252C} mutant, the incubation with insulin had little effect on the [^{3}H] thymidine incorporation into DNA (Fig. 8D), suggesting that DNA synthesis was poorly stimulated by insulin in these cells. In marked contrast, insulin evoked a 6.2-fold increase of thymidine incorporation in cells expressing the wild type IR (Fig. 8D). The basal incorporation of thymidine into DNA remained very low in cells expressing both the wild type or mutant form of the IR all along the 2 h of incubation at 37°C, indicating that the reduced ability of insulin to stimulate DNA synthesis was not related to a high basal activity.

In summary, the IR^{R252C} mutant demonstrated normal autophosphorylation and a normal ability to phosphorylate IRS-1 and IRS-2 as well as downstream substrates such as Akt/PKB. In contrast, the IR^{R252C} mutant displays a reduced ability to phosphorylate Shc, to activate downstream MAPKs (ERK1/2) as well as a reduced DNA synthesis in response to insulin as compared to the wild type IR.

Discussion

The identification of genetic mutations in patients with severe forms of insulin resistance has provided important insights into the structure and function of IR, as well as into the molecular mechanisms of insulin action [27]. In this study, we report a homozygous point mutation occurring in the cysteine-rich domain of the α-subunit expressed in cells from a patient suffering from a variant form of type A syndrome of insulin resistance and acanthosis nigricans. This insulin resistance was related to a considerable reduction of the number of IR present at the cell surface and to a more significant reduction of their affinity for insulin. Transfection of the mutant receptor in CHO cells enabled us to analyse in detail the consequences of this point mutation on the cell biology and signalling capacity of this receptor and to collect information on the cascade of events following insulin binding to its receptor. The studies revealed that, in comparison with IRwt, IR^{R252C} displays a slower rate of synthesis;

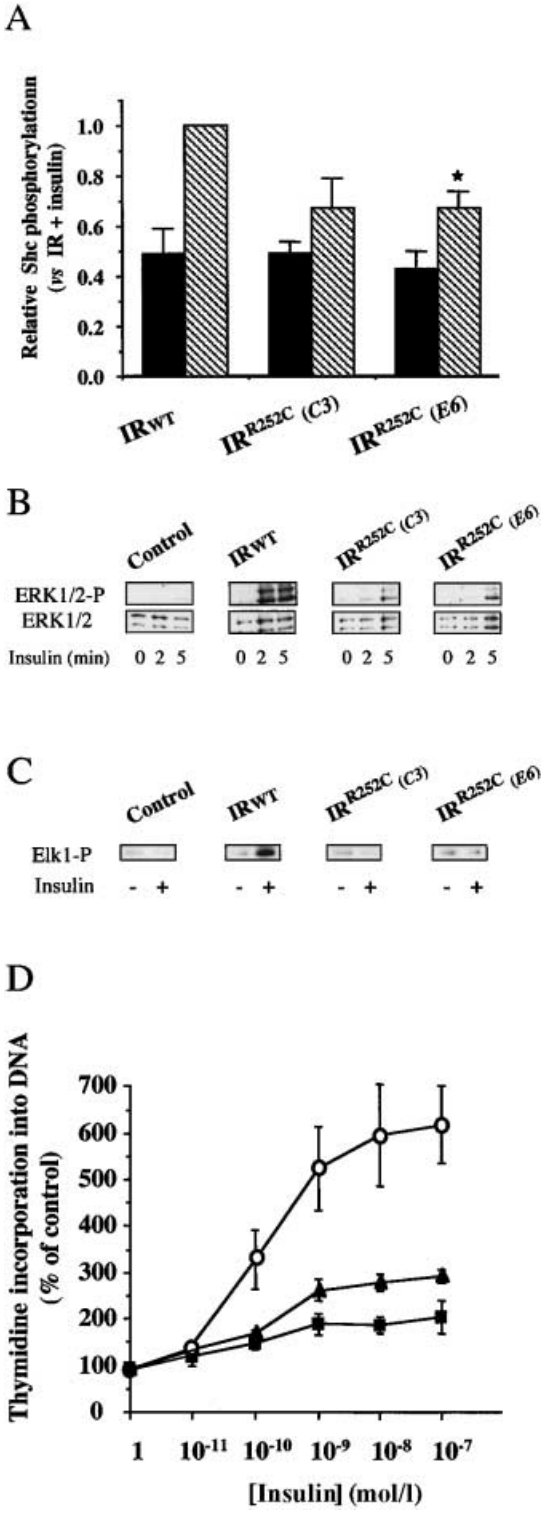

Fig. 8A–D. Insulin-induced activation of the MAPK pathway. **A** Insulin-induced phosphorylation of Shc. Following a 3 min incubation at 37°C in the presence of 10^{-7} mol/l insulin, cells were lysed in 1% Triton X-100 and Shc was immunoprecipitated and resolved on SDS-polyacrylamide gel. Phosphorylated Shc was detected with an anti-phosphotyrosine antibody. Results are expressed as mean ± SE of three independent experiments quantified by densitometry. *$p<0.01$. *solid bars* – insulin; *backed hatched bars* + insulin. **B** Insulin-induced phosphorylation of ERK1/2. Cells were treated with 10^{-7} mol/l insulin and ERK1/2 phosphorylation was detected as described in the Methods section. CHO cells with low endogenous levels of IR were used as a control. Results are representative of three independent experiments. **C** Insulin-induced activation of ERK1/2. Cells were treated with 10^{-7} mol/l insulin for 5 min at 37°C. After cell lysis, phosphorylation of Elk1 by ERK1/2 in cells expressing the IRwt or IR^{R252C} mutants was assessed as described in the Methods section. CHO cells with low endogenous expression of IR were used as a control. Results are representative of three independent experiments. **D** [^{3}H]-Thymidine incorporation into DNA. Insulin-induced [^{3}H] thymidine incorporation into DNA was measured as described in the Methods section. Each point was carried out in duplicate and the results represent the mean ± SE of three independent experiments. IRwt (*open circles*), IR^{R252C} clone E6 (*solid triangles*), IR^{R252C} clone C3 (*solid squares*)

Fig. 9. Position of Arg 252 and Cys 3 in the three dimensional structure of the insulin molecule. A model of the three N-terminal modules of the IR (L1-Cys-rich-L2) was generated by threading the IR amino acid sequence onto the 3-D structure of the equivalent modules of the IGF-I receptor determined by X-ray crystallography [43], using the Automated Protein Modelling Server Swiss-Model [44] running at the Glaxo-Wellcome Experimental Research in Geneva, Switzerland. The resulting structure is displayed using the program RasMol version 2.6 [45]. The receptor backbone is shown in *blue*, Cys 3 in *red*, Arg 252 in yellow

a close to abolition of insulin-induced internalisation; a normal capacity to be autophosphorylated, to phosphorylate both IRS 1 and IRS 2, to promote association of PI3 Kinase with IRS proteins and to activate Akt in response to insulin; and finally, a marked reduction of its capacity to induce Shc and ERK1/2 phosphorylation, to promote ERK1/2 activity and to incorporate thymidine into DNA in the presence of insulin.

The specific site of reduction in IR^{R252C} synthesis is unclear. Indeed, IR^{R252C} undergoes normal post-translational processing, ie the precursor is properly cleaved into α- and β-subunits; N-linked complex oligosaccharides are added to the polypeptide chains after proteolytic cleavage; and, finally, the IR are expressed on the cell surface as the α2β2 heterotetramer form. But these different maturation steps proceed at a slower rate in IR^{R252C} than in IRwt. These results are in agreement with previous studies showing that mutations in the N-terminal half of the α-subunit could impair intracellular transport [28, 29, 30, 31, 32, 33]. One possible interpretation of these events is a misfolding of the protein in the endoplasmic reticulum. It has been recently shown that folding of IR monomers was facilitated by molecular chaperones (calnexin and calreticulin) and occurred before homodimerisation [34]. Inhibition of these interactions by castanospermine accelerated IR dimerisation and resulted in the appearance of misfolded proreceptors whose processing was delayed and cell surface expression reduced. In those conditions, only a subset of receptors were transported to the cell surface while a pool of uncleaved receptors were retained in a pre-Trans Golgi network compartment. Similarly, the reduction in the number of IR^{R252C} at the cell surface in vivo and the marked reduction in the insulin binding might stem from the retention of misfolded and uncleaved proreceptors in the Golgi apparatus.

The recently determined structure of the first three N-terminal modules (L1-Cys-rich-L2) of the IGF-I receptor [35] that contain the major ligand binding site provides a plausible molecular explanation for the reduced affinity of IR^{R252C}. When the IR sequence is threaded upon this structure (Fig. 9), it is clear that ^{252}Arg (shown in yellow) is exposed in the putative ligand-binding central cavity between the three modules, in close proximity to the first cysteine of the sequence at position 3 (shown in red). The mutation of ^{252}Arg to Cys could favour the formation of an abnormal disulfide bond between ^{3}Cys and ^{252}Cys, that might lock the L1 module and Cys-rich module together into a conformation unfavourable for high affinity binding. Other mismatches with other cysteines from the Cys-rich region could also occur, especially with ^{253}Cys, resulting in a disturbed 3-D structure [36, 37, 38].

The decrease in the insulin-induced internalisation of IR^{R252C} is related to a reduced redistribution of the receptors from microvilli to the non-villous domains of the cell surface. Because IR^{R252C} is normally phosphorylated, the conformational change affecting the binding capacity of the receptor might also perturb other domains of the receptor known to participate in the control of IR movement in the plane of the membrane. In particular, this conformational change could affect the transmembrane domain of IR^{R252C} which has been shown to play a key role in the surface shift of IR [39].

The reduced surface redistribution of IR^{R252C} leads to an inhibition of IR^{R252C} internalisation which in turn results in a loss of insulin-induced receptor down-regulation and in an inhibition of insulin degradation. This is consistent with our previous observations regarding the consequences of insulin-IR complex endocytosis on these two parameters [40, 41]. In contrast, the decrease of insulin-IR complexes endocytosis is not accompanied by a loss of IRS 1/IRS 2 phosphorylation. These observations are in agreement with previous studies showing that IRS 1 phosphorylation is preserved at 4°C (a temperature at which IR endocytosis is prevented) [16, 17] as well as in cells expressing a dominant interfering dynamin which prevents clathrin-coated pits mediated endocytosis [15]. Along the same line, we have recently described a mutant IR (IR^{C860S}) capable of phosphorylating IRS 1 in spite of its defective internalisation. In addition, similarly to what is occurring in cells expressing IR^{R252C}, IRS 1 phosphorylation could be achieved by IR^{C860S} localised mainly on microvilli supporting the idea that some IR biological signals can be elicited from these surface domains. However, endosome could also be a site of IR signal transduction and biological responsiveness, as suggested by studies of the kinetics of IR kinase activation and of the subcellular localisation of this kinase domain [18, 19, 20, 42].

Despite the fact that IR^{R252C} shows a decreased affinity for insulin, its autophosphorylation in response to insulin, as well as the insulin-promoted phosphorylation of IRS 1/IRS 2 in cells expressing this mutant receptor (seen both by dose-response curves and kinetics of phosphorylation), remained in a range comparable to those recorded in cells expressing IRwt. Of note, the basal rate of IR^{R252C} and substrate phosphorylation were low, indicating that the intrinsic tyrosine kinase of the β-subunit and the two substrates are not constitutively activated in cells expressing the mutant receptors. Taken together with the recorded inhibition of IR^{R252C} internalisation in the same conditions, these observations support the concept of a relatively higher sensitivity to activation of the reduced number of IR^{R252C} present at the cell surface. Such relatively higher or prolonged phosphorylation of the IR^{R252C} or both and the two substrates could be related to the prolonged exposure of IR^{R252C} to insulin on the cell surface (particularly on microvilli), as well as to a reduced rate of dephosphorylation which might be relat-

ed to their cycling inside the cell. Thus, defective endocytic trafficking could lead to an enhancement of some biological responses which suggests that receptor-mediated endocytosis could be critical for attenuating receptor signalling as proposed many years ago [39] and supported by more recent observations regarding the epidermal growth factor receptor [43, 44, 45].

In contrast to IRS 1/IRS 2, the phosphorylation of another major substrate of the IR (Shc) is inhibited in cells transfected with IR^{R252C}. Opposite patterns of activation were similarly noted concerning the downstream effectors of these two different signalling pathways. Along the IRS pathway, p85 association with both IRS 1 and IRS 2 as well as Akt phosphorylation remained normal in IR^{R252C} expressing cells while along the Shc pathway, ERK1/2 phosphorylation as well as the ability to phosphorylate their substrate and thymidine incorporation in DNA were considerably reduced.

We are not in position of establishing whether this altered signalling results from abnormal receptor structure or from its altered endocytic process or both. The recent observation that inhibition of endocytosis by expression of a dominant interfering dynamin mutant has no effect on any insulin signalling pathways tested, including the Shc pathway, would support the first possibility [15]. On the other hand, present data would lend support to the observations that in the case of the EGF receptor, a subset of (but not all) signal transducers require the normal endocytic trafficking of the activated receptor for full activation [43]. The differences between the two studies (and therefore the two receptors concerned: insulin and the EGF receptor) in terms of the signalling pathways requiring endocytosis might reflect the receptor specificity in this respect and may be part of the explanation on how different receptors may signal differently even if they are making use of the same signalling pathways.

In summary, detailed analysis of the functioning of a naturally occurring mutant IR leading to an extreme insulin resistance proved very useful to decipher the insulin signalling pathway and to determine the relevance of its endocytosis in the transmission of some biological signals.

Acknowledgements. This work has been supported by grants: 31.53686.98 and 31.65392.01 from the Swiss National Science Foundation.

References

1. Sun XJ, Rothenberg P, Kahn CR et al. (1991) Structure of the insulin receptor substrate IRS-1 defines a unique signal transduction protein. Nature 352: 73–77
2. Sun XJ, Wang LM, Zhang Y et al. (1995) Role of IRS-2 in insulin and cytokine signalling. Nature 377: 173–177
3. Sciacchitano S, Taylor SI (1997) Cloning, tissue expression, and chromosomal localization of the mouse IRS-3 gene. Endocrinology 138: 4931–4940
4. Lavan BE, Lane WS, Lienhard GE (1997) The 60-kDa phosphotyrosine protein in insulin-treated adipocytes is a new member of the insulin receptor substrate family. J Biol Chem 272: 11439–11443
5. Lavan BE, Fantin VR, Chang ET, Lane WS, Keller SR, Lienhard GE (1997) A novel 160-kDa phosphotyrosine protein in insulin-treated embryonic kidney cells is a new member of the insulin receptor substrate family. J Biol Chem 272: 21403–21407
6. Smith-Hall J, Pons S, Patti ME et al. (1997) The 60 kDa IR substrate functions like an IRS protein (pp60IRS3) in adipose cells. Biochemistry 36: 8304–8310
7. Pronk GJ, McGlade J, Pelicci G, Pawson T, Bos JL (1993) Insulin-induced phosphorylation of the 46- and 52-kDa Shc proteins. J Biol Chem 268: 5748–5753
8. Levy-Toledano R, Taouis M, Blaettler DH, Gorden P, Taylor SI (1994) Insulin-induced activation of phosphatidyl inositol 3-kinase. Demonstration that the p85 subunit binds directly to the COOH terminus of the insulin receptor in intact cells. J Biol Chem 269: 31178–31182
9. White MF (1997) The insulin signalling system and the IRS proteins. Diabetologia 40 [Suppl 2]: S2–S17
10. Carpentier JL, Paccaud JP, Backer J, Gilbert A, Orci L, Kahn CR (1993) Two steps of insulin internalization depend on different domains of the Beta-subunit. J Cell Biol 118: 831–839
11. Hamer I, Renfrew-Haft CR, Paccaud JP, Maeder C, Taylor S, Carpentier JL (1997) Dual role of a dileucine motif in IR endocytosis. J Biol Chem 272: 21685–21691
12. Leconte I, Carpentier JL, Clauser E (1994) The functions of the human insulin receptor are affected in different ways by mutation of each of the four N-glycosylation sites in the beta subunit. J Biol Chem 269: 18062–18071
13. Yamamoto-Honda R, Kadowaki T, Momomura K et al. (1993) Normal insulin receptor substrate-1 phosphorylation in autophosphorylation-defective truncated insulin receptor. Evidence that phosphorylation of substrates might be sufficient for certain biological effects evoked by insulin. J Biol Chem 268: 16859–16865
14. Maggi D, Andraghetti G, Cordera R (1995) A Ser for Cys mutation in the extracellular portion of insulin receptor beta subunit impairs the insulin-IR complex internalization in CHO cells. Biochem Biophys Res Commun 210: 931–937
15. Ceresa BP, Kao AW, Santeler SR, Pessin, JE (1998) Inhibition of clathrin-mediated endocytosis selectively attenuates specific insulin receptor signal transduction pathways. Mol Cell Biol 18: 3862–3870
16. Heller-Harrison RA, Morin M, Czech MP (1995) Insulin regulation of membrane-associated insulin receptor substrate 1. J Biol Chem 270: 24442–24450
17. Biener Y, Feinstein R, Mayak M, Kaburagi Y, Kadowaki T, Zick Y (1996) Annexin II is a novel player in insulin signal transduction. Possible association between annexin II phosphorylation and insulin receptor internalization. J Biol Chem 271: 29489–29496
18. Kublaoui B, Lee J, Pilch PF (1995) Dynamics of signaling during insulin-stimulated endocytosis of its receptor in adipocytes. J Biol Chem 270: 59–65
19. Bevan AP, Burgess JW, Drake PG, Shaver A, Bergeron JJ, Posner BI (1995) Selective activation of the rat hepatic endosomal insulin receptor kinase. Role for the endosome in insulin signaling. J Biol Chem 270: 10784–10791
20. Inoue G, Cheatham B, Emkey R, Kahn CR (1998) Dynamics of insulin signaling in 3T3-L1 adipocytes. Differential compartmentalization and trafficking of insulin receptor substrate IRS-1 and IRS-2. J Biol Chem 273: 11548–11555

21. Kahn CR, Flier JS, Bar RS et al. (1976) The syndromes of insulin resistance and acanthosis nigricans. Insulin- receptor disorders in man. N Engl J Med 294: 739–745
22. Seino S, Seino M, Bell GI (1990) Human insulin-receptor gene. Diabetes 39: 129–133
23. Munson PJ, Rodbard D (1980) Ligand: a versatile computerized approach for characterization of ligand-binding systems. Anal Biochem 107: 220–239
24. Levy-Toledano R, Caro LHP, Hindman N, Taylor SI (1993) Streptavidin blotting: a sensitive technique to study cell surface proteins, application to investigate autophosphorylation and endocytosis of biotin-labeled IR. Endocrinology 133: 1803–1808
25. Hedo JA, Kahn CR, Hayashi M, Yamada KM, Kasuga M (1983) Biosynthesis and glycosylation of the insulin receptor. Evidence for a single polypeptide precursor of the two major subunits. J Biol Chem 258: 10020–10026
26. Kohn AD, Takeuchi F, Roth RA (1996) Akt, a pleckstrin homology domain containing kinase, is activated primarly by phosphorylation. J Biol Chem 271: 21920–21926
27. Taylor SI, Cama A, Accili D et al. (1992) Mutations in the insulin receptor gene. Endocr Rev 13: 566–595
28. Kadowaki T, Kadowaki H, Accili D, Taylor SI (1990) Substitution of lysine for asparagine at position 15 in the alpha-subunit of the human insulin receptor. A mutation that impairs transport of receptors to the cell surface and decreases the affinity of insulin binding. J Biol Chem 265: 19143–19150
29. Kadowaki T, Kadowaki H, Accili D, Yazaki Y, Taylor SI (1991) Substitution of arginine for histidine at position 209 in the alpha-subunit of the human insulin receptor. A mutation that impairs receptor dimerization and transport of receptors to the cell surface. J Biol Chem 266: 21224–21231
30. van der Vorm ER, van der Zon GC, Moller W, Krans HM, Lindhout D, Maassen JA (1992) An Arg for Gly substitution at position 31 in the insulin receptor, linked to insulin resistance, inhibits receptor processing and transport. J Biol Chem 267: 66–71
31. van der Vorm ER, Kuipers A, Kielkopf-Renner S, Krans HM, Moller W, Maassen JA (1994) A mutation in the IR that impairs proreceptor processing but not insulin binding. J Biol Chem 269: 14297–14303
32. Maassen JA, Van der Vorm ER, Van der Zon GC, Klinkhamer MP, Krans HM, Moller W (1991) A leucine to proline mutation at position 233 in the insulin receptor inhibits cleavage of the proreceptor and transport to the cell surface. Biochemistry 30: 10778–10783
33. Accili D, Frapier C, Mosthaf L, Lander E, Ullrich A, Taylor SI (1989) A mutation in the insulin receptor gene that impairs transport of the receptor to the plasma membrane and causes insulin-resistant diabetes. EMBO J 8: 2509–2517
34. Bass J, Chiu G, Argon Y, Steiner DF (1998) Folding of insulin receptor monomers is facilitated by the molecular chaperones calnexin and calreticulin and impaired by rapid dimerization. J Cell Biol 141: 637–646
35. Garrett TPJ, McKern NM, Lou M et al. (1998) Crystal structure of the first three domains of the type 1 insulin-like growth factor receptor. Nature 394: 395–399
36. De Meyts P (1994) The structural basis of insulin and insulin-like growth factor-I receptor binding and negative cooperativity, and its relevance to mitogenic versus metabolic signalling. Diabetologia 37 [Suppl 2]: S135
37. Peitsch MC (1996) ProMod and Swiss-Model Internet-based tools for automated comparative protein modelling. Biochem Soc Trans 24: 274–279
38. Sayle R, Milner-White EJ (1995) RasMol: Biomolecular graphics for all. TIBS 20: 374
39. Yamada K, Carpentier JL, Cheatham B, Goncalves E, Shoelson SE, Kahn CR (1995) Role of the transmembrane domain and flanking amino acids in internalization and down-regulation of the insulin receptor. J Biol Chem 270: 3115–3122
40. Carpentier JL, Dayer JM, Lang U, Silverman R, Orci L, Gorden P (1984) Down-regulation and recycling of IR. Effect of monensin on IM-9 lymphocytes and U-937 monocyte-like cells. J Biol Chem 259: 14190–14195
41. Geiger D, Carpentier JL, Gorden P, Orci L (1989) Down-regulation of insulin receptors is related to insulin internalization. Exp Cell Res 185: 33–40
42. Bevan AP, Krook A, Tikerpae J, Seabright PJ, Siddle K, Smith GD (1997) Chloroquine extends the lifetime of the activated insulin receptor complex in endosomes. J Biol Chem 272: 26833–26840
43. Vieira AV, Lamaze C, Schmid SL (1996) Control of EGF receptor signaling by clathrin-mediated endocytosis. Science 274: 2086–2089
44. Wells A, Welsh JB, Lazar CS, Wiley HS, Gill GN, Rosenfeld MG (1990) Ligand-induced transformation by a noninternalizing epidermal growth factor receptor. Science 247: 962–964
45. Masui H, Wells A, Lazar CS, Rosenfeld MG, Gill GN (1991) Enhanced tumorigenesis of NR6 cells which express non-down-regulating epidermal growth factor receptors. Cancer Res 51: 6170–6175